Tributyltin chloride induces chondrocyte damage through the activation of NLRP3-mediated inflammation and pyroptosis

SILONG XIA and RONG MA

Department of Orthopedics, The Affiliated Jianhu Hospital of Yangzhou University, Yancheng, Jiangsu 224700, P.R. China

Received February 6, 2024; Accepted April 11, 2024

DOI: 10.3892/mmr.2024.13247

Abstract. Tributyltin chloride (TBTC) is known to have effects and mechanisms in various diseases; however, whether TBTC is detrimental to joints and causes osteoarthritis (OA), as well as its underlying mechanism, has not yet been fully elucidated. The present study explored the effects of TBTC on rat chondrocytes, as well as on mouse OA. The toxicity of TBTC toward rat chondrocytes was detected using a lactate dehydrogenase (LDH) leakage assay and cell viability was evaluated using the Cell Counting Kit-8 assay. The results showed that TBTC decreased the viability of rat chondrocytes and increased the LDH leakage rate in a concentration-dependent manner. Moreover, compared with in the control group, TBTC increased the expression levels of interleukin (IL)-1β, IL-18, matrix metalloproteinase (MMP)-1, MMP-13, NLR family pyrin domain containing 3 (NLRP3), caspase-1, PYD and CARD domain containing, and gasdermin D in chondrocytes. Furthermore, knockdown of NLRP3 reversed the TBTC-induced increases in LDH leakage and NLRP3 inflammasome-associated protein levels. *In vivo*, TBTC exacerbated cartilage tissue damage in mice from the OA group, as evidenced by the attenuation of safranin O staining. In conclusion, TBTC may aggravate OA in mice by promoting chondrocyte damage and inducing pyroptosis through the activation of NLRP3 and caspase-1 signaling. The present study demonstrated that TBTC can cause significant damage to the articular cartilage; therefore, TBTC contamination should be strictly monitored.

Introduction

Osteoarthritis (OA) is the most common joint disease in the world, with a prevalence of ~10% of the population (1). The characteristic structural changes include synovial inflammation, a loss of articular cartilage, subchondral bone changes, meniscal injuries, and tendon and ligament degeneration (2). OA is the leading cause of joint pain, loss of function and disability in older adults, with the knee being the most commonly affected joint (3). The pathogenesis of OA has not yet been clarified, but previous studies have suggested that inflammation, pyroptosis and apoptosis serve important roles in the progression of OA (3,4).

The NLR family pyrin domain containing 3 (NLRP3) inflammasome has become the most widely studied inflammasome in recent years, and it can be activated by various pathogenic events, such as reactive oxygen species generation, mitochondrial dysfunction and numerous types of pathogens, such as bacteria and viruses (5). The NLRP3 inflammasome has an important role in inflammatory bowel disease, cardiovascular disease, diabetes mellitus, autoimmune disease and lung disease (5-7). Previous studies have shown that the NLRP3 inflammasome is widely involved in the development of OA (8,9). Therefore, targeting the NLRP3 inflammasome may be considered an important strategy for the treatment of OA. For example, in chondrocytes, icariin antagonizes NLRP3 inflammasome-mediated activation of caspase-1 signaling, thereby attenuating inflammation during osteoporosis (10). In addition, the use of n-3 polyunsaturated fatty acid (PUFA)-enriched diets has been shown to protect mice from obesity-associated post-traumatic OA, and an in-depth study revealed that this phenomenon is related to the inhibition of NLRP3/caspase-1 signaling by PUFAs (11).

Tributyltin (TBT) was once widely used as an antifouling paint for ships; however, it was subsequently found to cause serious harm to marine organisms, especially mollusks, and it was thus banned globally in 2003 (12). Owing to its long-term residue, even after a long period of time, TBT still exists in seawater and sediments; it can therefore accumulate in marine organisms and is still present after cooking, thus suggesting that the consumption of seafood may be a potential TBT hazard (13,14). TBT chloride (TBTC) is the main form of TBT present in water. Studies have shown that TBTC is an endocrine disruptor in mammals and can affect the reproductive function of animals (12,15). However, the understanding of the effects of TBTC on the articular cartilage remains limited. The present study explored the effects and molecular mechanisms of TBTC on chondrocytes *in vitro* and *in vivo* to reveal the potential effects of TBTC on joint damage.

Correspondence to: Dr Rong Ma, Department of Orthopedics, The Affiliated Jianhu Hospital of Yangzhou University, 666 Nanhuan Road, Yancheng, Jiangsu 224700, P.R. China
E-mail: qinliyou1170@163.com

Key words: tributyltin chloride, NLRP3 inflammasome, pyroptosis, cartilage damage

Materials and methods

Rat chondrocyte culture. Rat primary chondrocytes (cat. no. CP-R087) were obtained from Procell Life Science & Technology Co., Ltd. The cells were suspended in rat chondrocyte complete medium (cat. no. CM-R087; Procell Life Science & Technology Co., Ltd.) supplemented with 10% fetal bovine serum (Thermo Fisher Scientific, Inc.) and 100 U/ml penicillin-100 μg/ml streptomycin (penicillin-streptomycin liquid; Beijing Solarbio Science & Technology Co., Ltd.), and were incubated at 37˚C in 5% CO_2. The cells were divided into control, low-concentration (25 nM) TBTC (MilliporeSigma), medium-concentration (50 nM) TBTC and high-concentration (100 nM) TBTC groups at 37˚C for 24 h. The experiments were repeated three times for each group.

Cell Counting Kit-8 (CCK-8) assay. The cells were resuspended and seeded in 96-well plates at a density of $1x10^4$ cells/well. When the cells reached 50-60% confluence, the medium was discarded, and TBTC was added at final concentrations of 0, 25, 50 and 100 nM for 24 h at 37˚C. The cells were then incubated with CCK-8 reagent (Beijing Solarbio Science & Technology Co., Ltd.) for 1 h at 37˚C and the absorbance values were determined at 450 nm.

Western blotting. The cells were lysed with RIPA buffer (high; Beijing Solarbio Science & Technology Co., Ltd.) and the lysate was centrifuged at 11,000 x g for 15 min at 4˚C, after which the supernatant was collected. The protein concentration was quantified using a BCA protein assay kit (Beijing Solarbio Science & Technology Co., Ltd.), and proteins (20 μg) were separated by SDS-PAGE on 10% gels. The proteins were then transferred to PVDF membranes, which were incubated with 5% nonfat milk for 1 h at 37˚C. Subsequently, primary antibodies against β-actin (1:1,000; cat. no. 4970; Cell Signaling Technology, Inc.), NLRP3 (1:1,000; cat. no. ab263899; Abcam), interleukin (IL)-1β (1:1,000; cat. no. ab315084; Abcam), IL-18 (1:1,000; cat. no. ab223293; Abcam), matrix metalloproteinase (MMP)-1 (1:500; cat. no. 70R-50066; AmyJet Scientific, Inc.), MMP-13 (1:1,000; cat. no. ab219620; Abcam), caspase-1 (1:1,000; cat. nos. ab286125 for rat or ab138483 for mouse; Abcam), PYD and CARD domain containing (ASC; 1:1,000; cat. no. ab307560; Abcam) and gasdermin D (GSDMD; 1:1,000; cat. no. ab219800; Abcam) were incubated with the PVDF membranes overnight at 4˚C. The membranes were then incubated with an HRP-labeled goat anti-rabbit IgG (H+L) secondary antibody (1:3,000; cat. no. A0208 Beyotime Institute of Biotechnology) at room temperature for 1 h. After washing the membranes three times with TBS-Tween (0.1%), the protein bands were detected using an ECL western blotting substrate (Beijing Solarbio Science & Technology Co., Ltd.). The intensities of the protein bands were analyzed using ImageJ 1.8.0 software (National Institutes of Health), and the relative protein expression levels were calculated using β-actin as a reference.

Lactate dehydrogenase (LDH) leakage rate assay. Rat primary chondrocytes ($1x10^6$ cells/well in a 6-well plate) were divided into control, low-concentration (25 nM) TBTC, medium-concentration (50 nM) TBTC and high-concentration (100 nM) TBTC groups and were treated at 37˚C for 24 h. Cytotoxicity was evaluated by determining the LDH leakage rate in cell supernatants using a cytotoxicity LDH assay kit (MedChemExpress) according to the manufacturer's instructions.

Immunofluorescence (IF). Rat primary chondrocytes ($1x10^6$ cells/well in a 6-well plate) were divided into control, low-concentration (25 nM) TBTC, medium-concentration (50 nM) TBTC and high-concentration (100 nM) TBTC groups and were treated at 37˚C for 24 h. The chondrocytes were fixed with 4% paraformaldehyde (Beijing Solarbio Science & Technology Co., Ltd.) at room temperature for 20 min and then blocked with 5% donkey serum at room temperature for 2 h (Beijing Solarbio Science & Technology Co., Ltd.). Subsequently, the cells were incubated with a primary antibody against NLRP3 (1:50; cat. no. ab263899; Abcam) or GSDMD (1:50; cat. no. ab219800; Abcam) at 4˚C overnight. After being washed three times with PBS, the slides were incubated with Alexa Fluor 350-labeled goat anti-rabbit IgG (H+L) (1:200; cat. no. A0408; Beyotime Institute of Biotechnology) at room temperature for 1 h, followed by incubation with antifade mounting medium containing DAPI (Beyotime Institute of Biotechnology). Images were observed under a fluorescence microscope (magnification, x20; Olympus Corporation).

Cell cycle assay. Rat primary chondrocytes ($1x10^6$ cells/well in a 6-well plate) were divided into control, low-concentration (25 nM) TBTC, medium-concentration (50 nM) TBTC and high-concentration (100 nM) TBTC groups and were treated at 37˚C for 24 h. The cell cycle assay was performed using the DNA Content Quantitation Assay (Cell Cycle) (cat. no. CA1510; Beijing Solarbio Science & Technology Co., Ltd.). Briefly, cells were collected and fixed with 70% precooled ethanol (500 μl) at 4˚C overnight. The cells were then centrifuged at 800 x g at 4˚C for 15 min, 100 μl RNase A solution was added to the cell precipitate and the resuspended cells were incubated in a water bath at 37˚C for 30 min. Subsequently, 400 μl PI staining solution was added to the cell suspension, which was incubated at 4˚C for 30 min in the dark. Finally, the cells were analyzed using a BD FACSCanto II flow cytometer (BD Biosciences) and data analysis was performed using FlowJo 10 software (FlowJo, LLC).

EdU staining. Rat primary chondrocytes ($1x10^6$ cells/well in a 6-well plate) were divided into control, low-concentration (25 nM) TBTC, medium-concentration (50 nM) TBTC and high-concentration (100 nM) TBTC groups and were treated at 37˚C for 24 h. EdU staining was performed using an EdU cell proliferation assay kit (Shanghai Recordbio Biological Technology). Rat primary chondrocytes ($1x10^6$ cells/well in a 6-well plate) were incubated with 50 μM EdU (20 μl total volume) for 2 h at 37˚C. After three washes with PBS, the cells were incubated with 4% paraformaldehyde for 15 min at room temperature and then with 0.5% Triton X-100 for 15 min at room temperature. Subsequently, the samples were blocked with antifade mounting medium containing DAPI (Beyotime Institute of Biotechnology) and were observed under a fluorescence microscope (Olympus Corporation). Cell proliferation rate was calculated as follows:

Cell proliferation rate (%)=EdU-positive cells/DAPI-positive cells x100.

Animal grouping and an OA mouse model. The present study used rat primary chondrocytes *in vitro* and a mouse model *in vivo*. The present study aimed to verify that TBTC damaged articular chondrocytes in different species and, compared with rat models, mouse models are easier to generate and are less costly. C57BL/6J male mice [n=20; Shulaibao (Wuhan) Biotechnology Co., Ltd.] were acclimated for 1 week at 22-24˚C and 45% humidity. All mice were given free access to food and water under a 12-h light/dark cycle. All mice were randomly divided into the following four groups: Control, OA, TBTC and TBTC + OA groups (n=5 mice/group). The mouse OA model was induced by injection of monosodium iodoacetate (MIA; cat. no. I2512; MilliporeSigma) as previously described (16). Specifically, MIA was dissolved in a 0.9% NaCl solution to a final concentration of 60 mg/ml, and 50 μl MIA solution was injected into the right knee joint cavity of the mice in the OA groups. The control mice were injected with 50 μl 0.9% NaCl solution. After 2 weeks of modeling, the OA model mice were further divided into two groups: In the TBTC group, the mice were injected with 50 μl 0.9% NaCl solution and were also administered TBTC daily at a dose of 10 μg/kg for 2 weeks, and in the other groups, the mice were administered an equal volume of saline for a total of 2 weeks. All of the mice were euthanized at the termination of the experiment, ensuring minimal suffering. No mice died naturally during the study. All mice were monitored twice daily for signs of discomfort, illness or distress by trained personnel. To minimize suffering and distress, isoflurane was utilized at an induction concentration of 5% and a maintenance concentration of 2% prior to cervical dislocation. Humane endpoints were established based on the guidelines from the Institutional Animal Care and Use Committee of Yangzhou University, and included >20% weight loss or gain, inability to eat or drink, persistent lack of mobility, signs of severe and chronic pain, and any conditions notably interfering with daily activities. When the mice were fully unresponsive to nociceptive stimuli indicating that they were fully anesthetized, cervical dislocation was used for euthanasia. Death was verified by the absence of respiration, heartbeat and reflexes. The knee joint tissues were subsequently collected.

Safranin O-Fast Green staining. Cartilage sections (1.0x1.0x0.5 cm) were cut from the mouse subchondral bone and fixed in 4% formaldehyde (Beijing Solarbio Science & Technology Co., Ltd.) for 3 days at 4˚C. Subsequently, the sections were decalcified in a 30% formic acid solution for 14 days at room temperature, dehydrated in an increasing ethanol gradient, embedded in paraffin and cut into 5-μm sections. The sections were stained using the modified Safranin-O and Fast Green stain kit (for bone) (Beijing Solarbio Science & Technology Co., Ltd.) according to the manufacturer's instructions. Finally, the sections were blocked with neutral gum (Beijing Solarbio Science & Technology Co., Ltd.). Normal cartilage was red in color, and the background was green, and staining was observed under a light microscope (Olympus Corporation).

Hematoxylin and eosin (H&E) staining. Cartilage samples were cut into 5-μm sections as aforementioned and were incubated using a H&E stain kit (Beijing Solarbio Science & Technology Co., Ltd.) according to the manufacturer's instructions. Briefly, the sections were incubated with hematoxylin at room temperature for 10 min, rinsed in tap water, and then stained with eosin at room temperature for 30 sec. After rinsing in tap water, and following dehydration, clearing and sealing, the sections were observed under a light microscope (Olympus Corporation).

Toluidine blue staining. Cartilage samples were cut into 5-μm sections as aforementioned and were deparaffinized and stained with a 1% toluidine blue O solution (Beijing Solarbio Science & Technology Co., Ltd.) for 20 min at 55˚C, according to the manufacturer's instructions. After being rinsed with distilled water, the sections were dehydrated with 95% ethanol, cleared with xylene and blocked with resin. Subsequently, the tissues were observed under a light microscope (Olympus Corporation).

Reverse transcription-quantitative PCR (RT-qPCR). Rat primary chondrocytes ($1x10^6$ cells/well in a 6-well plate) were divided into control, low-concentration (25 nM) TBTC, medium-concentration (50 nM) TBTC and high-concentration (100 nM) TBTC groups and were treated at 37˚C for 24 h. Total RNA was extracted from chondrocytes using TRIzol® reagent (Invitrogen; Thermo Fisher Scientific, Inc.) and was reverse transcribed into cDNA using PrimeScript™ RT master mix (cat. no. RR036A; Takara Bio, Inc.) according to the manufacturer's protocol. qPCR was performed on an ABI StepOnePlus real-time fluorescence qPCR instrument (Thermo Fisher Scientific, Inc.) using the SYBR® Select master mix (Beijing Think-Far Technology Co., Ltd.). The thermocycling conditions were as follows: Denaturation at 95˚C for 30 sec, followed by 35 cycles of annealing at 60˚C for 1 min and extension at 95˚C for 5 sec. The sequences of the primers used were as follows: NLRP3, forward 5'-ATAGCG TCATACGGGGGAAG-3', reverse 5'-CACCCACGGGCA AGATGAAA-3'; GAPDH, forward 5'-TGAGGAGTCCCC ATCCCAAC-3' and reverse 5'-ATGGTATTCGAGAGAAGG GAGG-3'. Relative gene expression was calculated using the $2^{-\Delta\Delta Cq}$ method (17) with GAPDH as an internal control.

Small interfering RNA (siRNA) transfection. The siRNA targeting NLRP3 (sense 5'-AAUUUAAAUACAUUUCAC CCA-3'; antisense 5'-TGGGTGAAATGTATTTAAATT-3') and the negative control (NC) siRNA (sense 5'-UUCUCC GAACGUGUCACGUUU-3'; antisense 5'-AAACGUGAC ACGUUCGGAGAA-3') were purchased from Shanghai GenePharma Co., Ltd. Briefly, primary rat chondrocytes ($1x10^6$ cells/well in a 6-well plate) were transfected with si-NLRP3 or NC at a final concentration of 20 nM using Lipofectamine® 3000 (Invitrogen; Thermo Fisher Scientific, Inc.) at 37˚C for 24 h, according to the manufacturer's instructions before TBTC treatment. Subsequently, the cells were collected immediately for subsequent experiments.

Statistical analysis. SPSS 18.0 statistical software (SPSS, Inc.) was used for data analysis and all experiments were repeated at least three times. The data are presented as

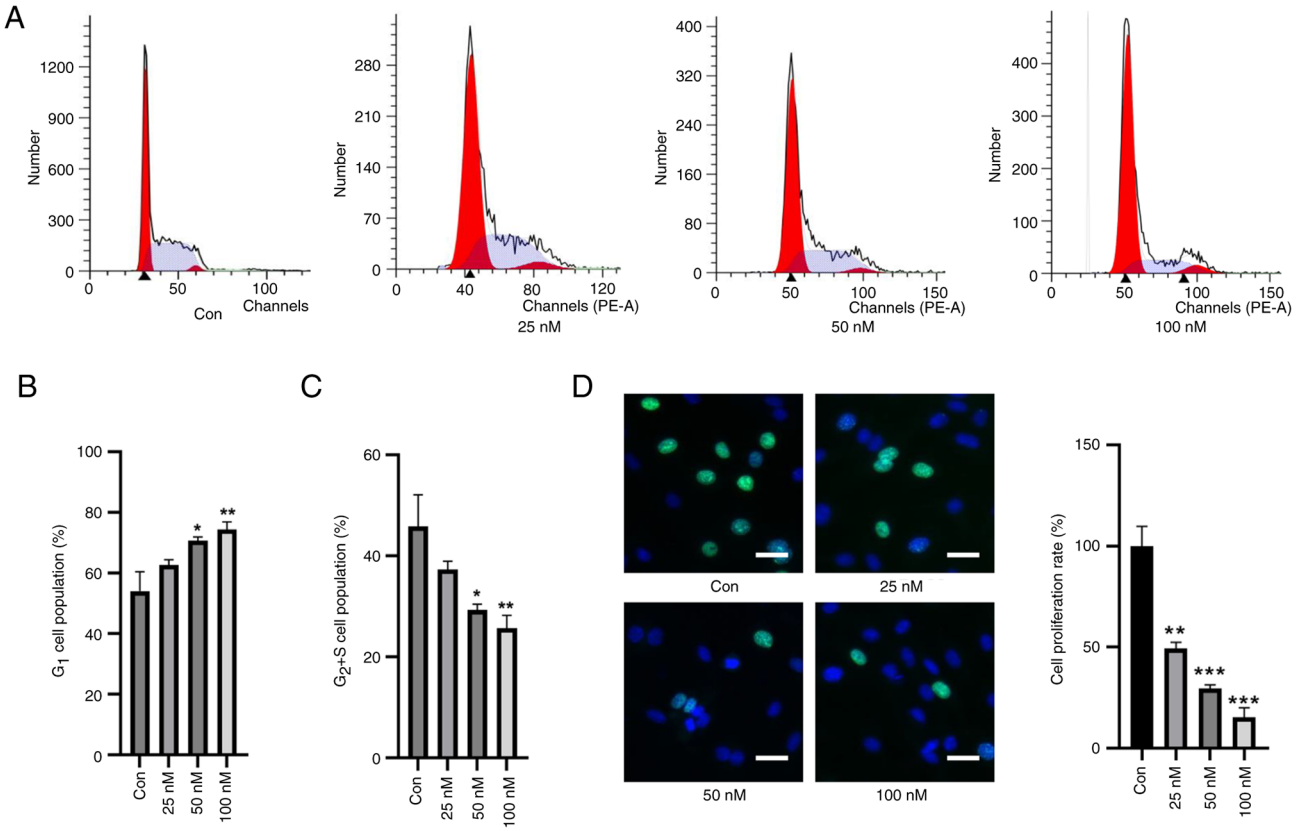

Figure 1. TBTC inhibits rat chondrocyte proliferation. (A) Flow cytometry showed that TBTC inhibited rat chondrocyte proliferation in a concentration-dependent manner. (B) Statistical analysis of G_1 cell population. (C) Statistical analysis of G_2 + S cell population. (D) EdU staining showed that TBTC inhibited rat chondrocyte proliferation (scale bar, 10 μm). *P<0.05, **P<0.01, ***P<0.001 vs. Con. Con, control; TBTC, tributyltin chloride.

the mean ± standard deviation. Differences among more than two groups were examined by one-way ANOVA, followed by Tukey's post hoc test. P<0.05 was considered to indicate a statistically significant difference.

Results

TBTC inhibits rat chondrocyte proliferation. First, the effects of TBTC on the cell cycle of rat chondrocytes were explored. Compared with in the control group, TBTC increased the number of cells in G_1 phase in a concentration-dependent manner and decreased the number of cells in the G_2 and S phases (Fig. 1A-C). EdU staining also showed that the proliferation of rat chondrocytes was significantly inhibited in response to an increasing concentration of TBTC (Fig. 1D). These results preliminarily suggested that TBTC was detrimental to the proliferation of rat chondrocytes.

TBTC induces rat chondrocyte injury. The CCK-8 assay results showed that TBTC reduced rat chondrocyte viability in a concentration-dependent manner (Fig. 2A). LDH leakage is the main indicator of pyroptosis, and LDH leakage was significantly greater in the TBTC groups than that in the control group (Fig. 2B). Furthermore, the mRNA expression levels of NLRP3 in rat chondrocytes in the TBTC group were significantly greater than those in the control group (Fig. 2C). After incubation with TBTC, the protein expression levels of NRLP3, IL-1β, IL-18, MMP-1 and MMP-13 in rat chondrocytes were significantly greater than those in the control group (Fig. 2D). These results suggested that TBTC serves a critical role in the destruction of chondrocytes by activating the NLRP3 inflammasome.

TBTC activates NLRP3 and caspase-1 signaling in rat chondrocytes. IF experiments revealed that the expression of NLRP3 and GSDMD was significantly greater in rat chondrocytes in the TBTC groups than that in the control group (Fig. 3A). Moreover, western blot analysis revealed that the expression levels of caspase-1, ASC and GSDMD were significantly elevated in the TBTC groups compared with those in the control group (Fig. 3B), indicating the induction of pyroptosis by TBTC in rat chondrocytes.

TBTC induces rat chondrocyte pyroptosis through the activation of NLRP3 signaling. To further verify whether TBTC induces rat chondrocyte pyroptosis via NLRP3, cells were transfected with a siRNA specifically targeting NLRP3. The siRNA targeting NLRP3 effectively inhibited NLRP3 expression compared with NC group (Fig. 4A). Compared with that in the TBTC group, the LDH leakage rate was significantly decreased in the si-NLRP3 + TBTC group (Fig. 4B). Moreover, the expression levels of pyroptosis-related proteins, including caspase-1, ASC and GSDMD, were significantly reduced in the si-NLRP3 + TBTC group than those in the TBTC group (Fig. 4C). These results suggested that TBTC induced rat chondrocyte pyroptosis by activating NLRP3 signaling.

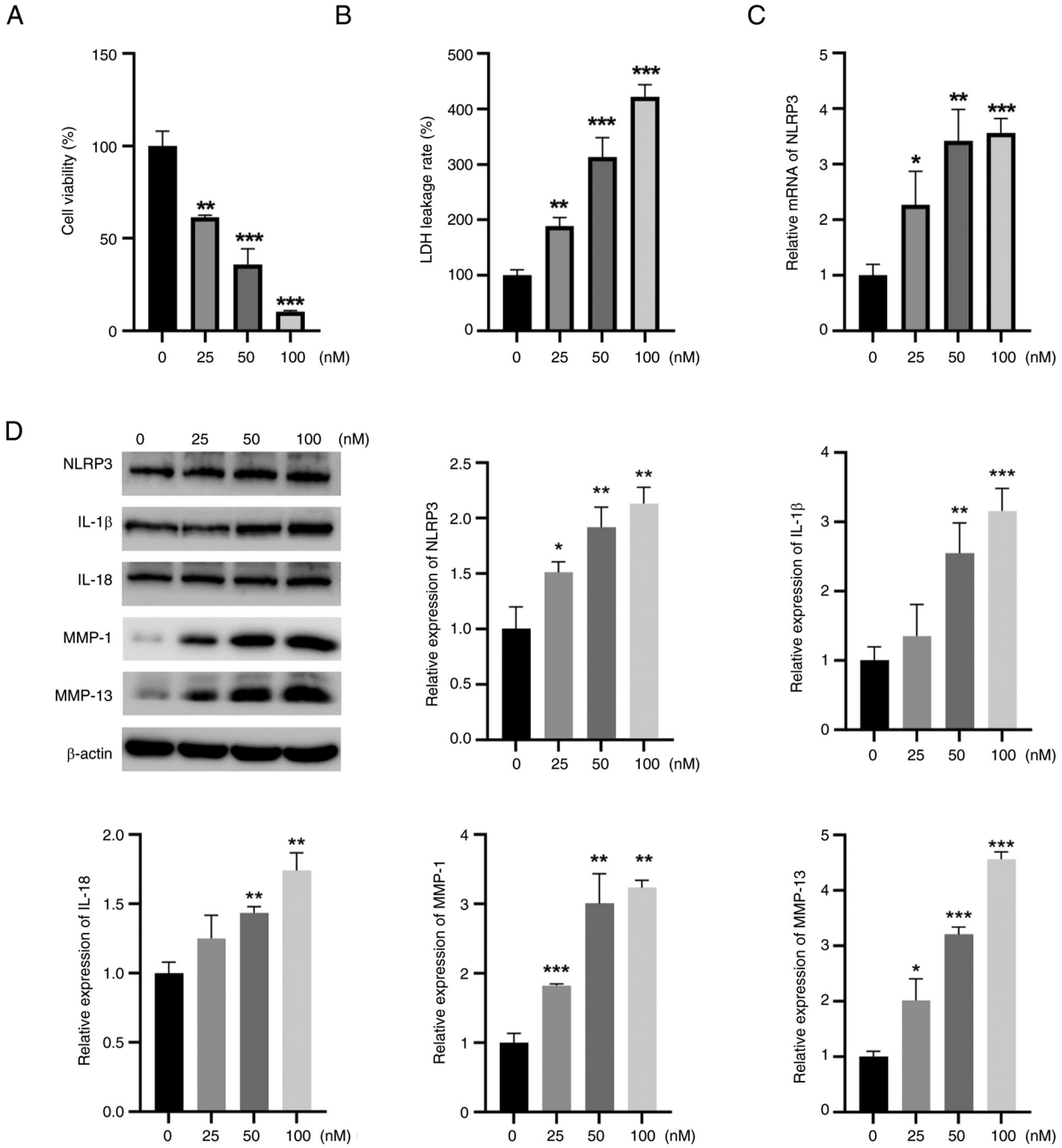

Figure 2. TBTC induces chondrocyte damage in rats. (A) Cell Counting Kit-8 results showed that TBTC reduced rat chondrocyte viability in a concentration-dependent manner. (B) TBTC significantly increased LDH leakage from rat chondrocytes. (C) Reverse transcription-quantitative PCR results revealed that TBTC elevated NLRP3 mRNA expression levels. (D) Western blot analysis results revealed that TBTC upregulated the protein expression levels of NLRP3, IL-1β, IL-18, MMP-1 and MMP-13 in rat chondrocytes. *P<0.05, **P<0.01, ***P<0.001 vs. Con. Con, control; IL, interleukin; LDH, lactate dehydrogenase; MMP, matrix metalloproteinase; NLRP3, NLR family pyrin domain containing 3; TBTC, tributyltin chloride.

TBTC enhances cartilage damage in the joints of mice from the OA group. H&E staining showed that in the cartilage of the control group, the cell nuclei were dark blue, the cytoplasm and cartilage matrix were pink, and the coloring was homogeneous; the surface of the cartilage was smooth and flat, and was arranged parallel to the surface of the joint (Fig. 5A). In the OA group, the surface of the cartilage was rough, the integrity of the cartilage was disrupted, and the surface cartilage exhibited fibrotic degeneration and defects. In the TBTC-treated group, the cartilage surface also showed some defects. Moreover, the integrity of the cartilage was markedly disrupted, and the cartilage defects were more pronounced in the TBTC + OA group (Fig. 5A). The results of Safranin O-Fast Green staining showed that the cartilage matrix was intact in the control group, as evidenced by proteoglycans stained in red, and by fibers,

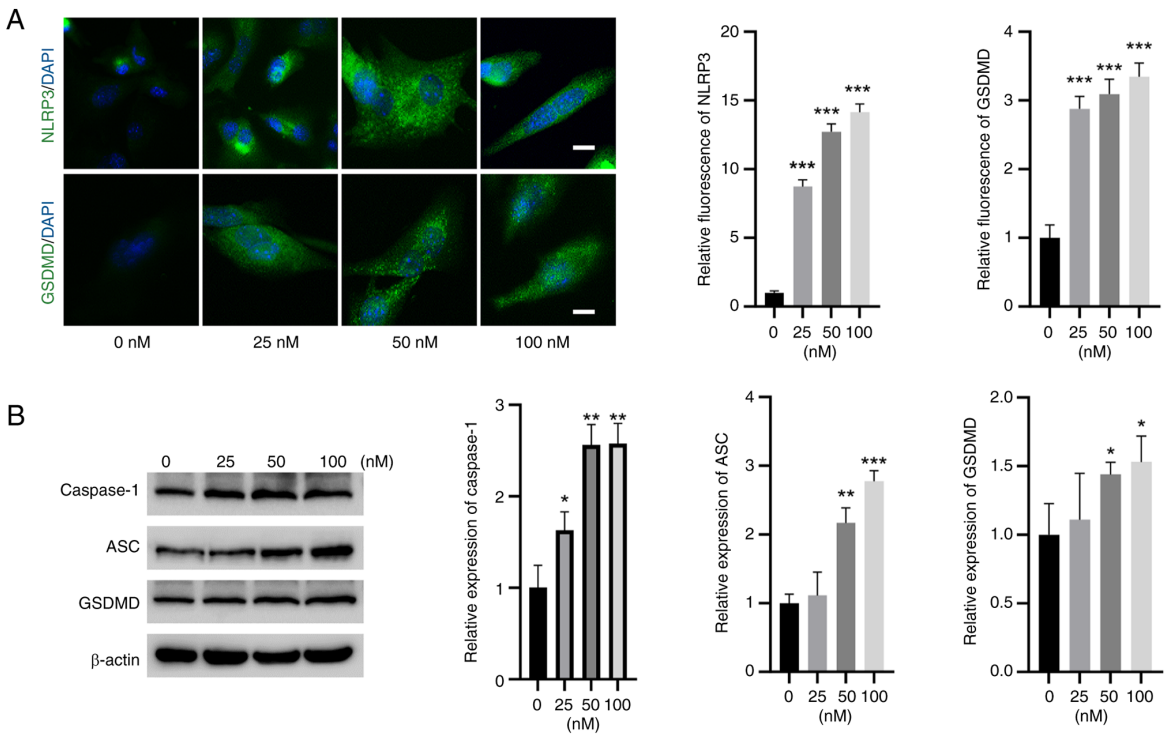

Figure 3. TBTC activates NLRP3 and caspase-1 signaling in rat chondrocytes. (A) Immunofluorescence experiments confirmed that TBTC increased the expression of NLRP3 and GSDMD in rat chondrocytes (scale bar, 5 μm). (B) Western blot analysis results showed that TBTC increased the expression levels of caspase-1, ASC and GSDMD in rat chondrocytes. *P<0.05, **P<0.01, ***P<0.001 vs. Con. ASC, PYD and CARD domain containing; Con. Con, control; GSDMD, gasdermin D; NLRP3, NLR family pyrin domain containing 3; TBTC, tributyltin chloride.

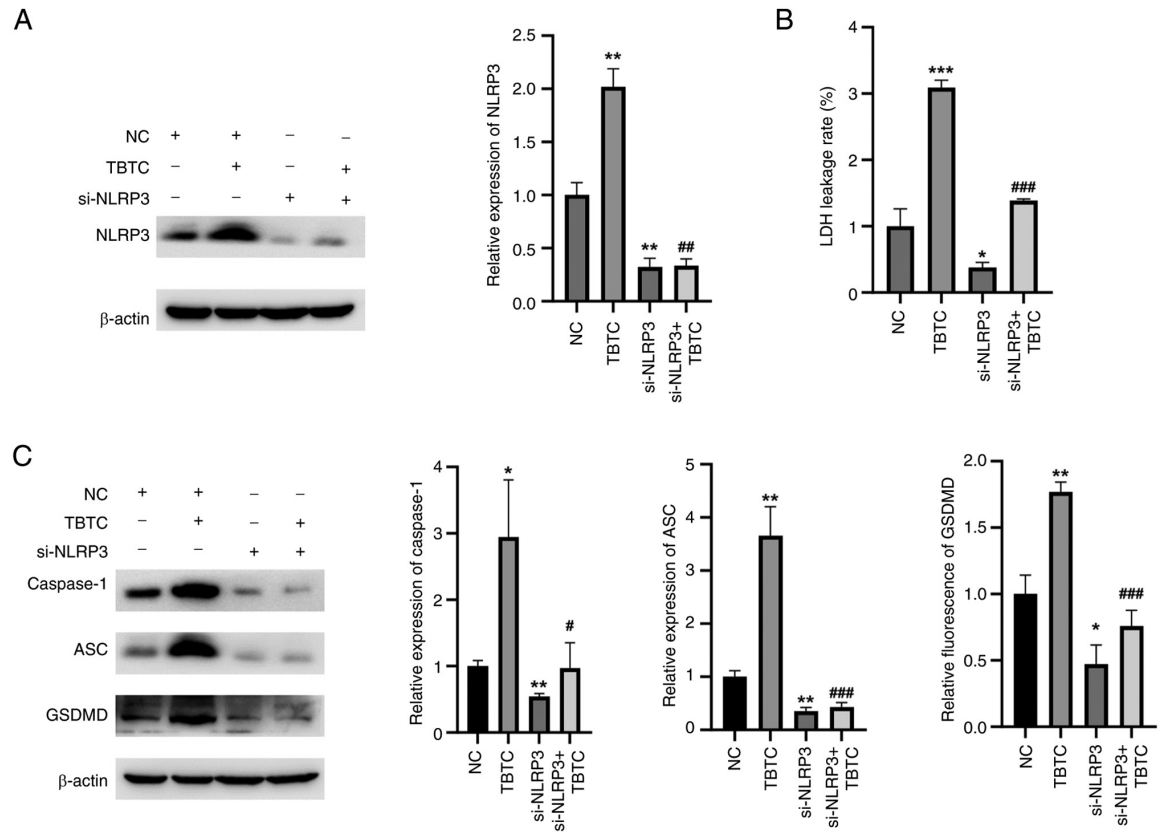

Figure 4. TBTC induces rat chondrocyte pyroptosis by activating NLRP3 signaling. (A) Western blot analysis revealed that si-NLRP3 could effectively inhibit the protein expression levels of NLRP3 in rat chondrocytes compared with that of the negative control. (B) Knockdown of NLRP3 inhibited the TBTC-induced increase in LDH leakage. (C) Compared with TBTC treatment, silencing NLRP3 reduced the expression levels of pyroptosis-related proteins. *P<0.05, **P<0.01, ***P<0.001 vs. NC; $^{\#}$P<0.05, $^{\#\#}$P<0.01, $^{\#\#\#}$P<0.001 vs. TBTC. ASC, PYD and CARD domain containing; Con. Con, control; GSDMD, gasdermin D; LDH, lactate dehydrogenase; NC, negative control; NLRP3, NLR family pyrin domain containing 3; si, small interfering; TBTC, tributyltin chloride.

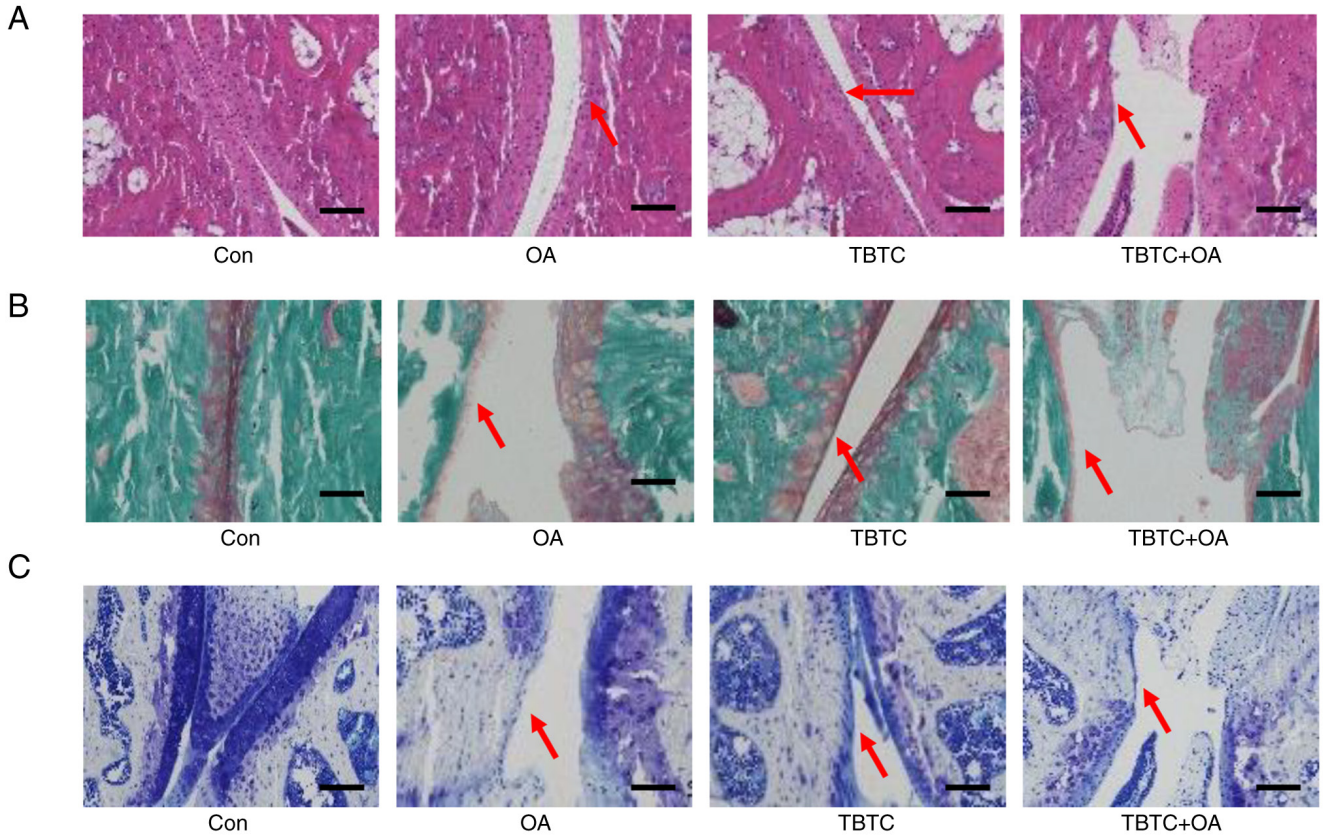

Figure 5. TBTC enhances cartilage damage in the osteoarticular joints of mice in the OA group. (A) Hematoxylin and eosin staining. (B) Safranin O-Fast Green staining. (C) Toluidine blue staining (magnification, x40, for all images; scale bar, 50 μm; red arrows indicate injured areas). Con. Con, control; OA, osteoarthritis; TBTC, tributyltin chloride.

the subchondral bone cortex and trabeculae stained in green (Fig. 5B). In the OA and TBTC groups, the cartilage matrix exhibited some degree of disruption, as evidenced by reduced proteoglycan coloration. In the TBTC + OA group, the reduction in proteoglycan coloring was further exacerbated (Fig. 5B). Toluidine blue staining also revealed greater articular cartilage degeneration in the mice from the OA and TBTC groups than in those from the control group (Fig. 5C). This cartilage degeneration was more pronounced in the mice from the TBTC + OA group (Fig. 5C). These results suggested that TBTC enhanced articular cartilage degeneration in a mouse model of OA.

TBTC enhances the NLRP3-mediated inflammatory response and pyroptosis in OA mouse bone joints. The present study then examined the effects of TBTC on cartilage tissue damage in mice. The results revealed that the protein expression levels of NLRP3, IL-1β, IL-18, MMP-1 and MMP-13 were significantly greater in the OA and TBTC groups than those in the control group (Fig. 6A). Similarly, the proteins were also upregulated in the TBTC + OA group (Fig. 6A). The expression levels of pyroptosis-related proteins were also detected. Notably, the expression levels of the pyroptosis-related proteins caspase-1, ASC and GSDMD were significantly greater in the OA and TBTC groups than those in the control group (Fig. 6B). These proteins were also increased in the TBTC + OA group (Fig. 6B). These results confirmed that TBTC could increase the NLRP3-mediated inflammatory response and pyroptosis, thereby promoting osteoarticular injury in mice.

Discussion

TBT is a synthetic metal compound and an important industrial raw material that is widely used as a stabilizer for plastic products, a pesticide, a fungicide, and an anticorrosive and antifouling coating for ships and boats (18). In the past 20 years, TBT has entered the environment, particularly the marine environment, in large quantities, resulting in widespread pollution of the oceans (18). TBT pollution has attracted the attention of a number of countries worldwide, and some countries have begun to take measures to limit the use of TBT. Studies have shown that TBT not only has endocrine-disrupting effects on organisms and causes reproductive toxicity, but also affects the nervous and immune systems (15,19,20). A previous study revealed that TBTC reduces the bone mineral density in the rat femoral epiphysis by inhibiting Wnt/β-catenin signaling, which in turn disrupts the homeostasis between osteogenesis and adipogenesis (21). However, the effects of TBTC on chondrocytes are still poorly understood.

To the best of our knowledge, for the first time, the present study revealed that TBTC decreased the survival of rat chondrocytes in a concentration-dependent manner. In addition, TBTC increased the leakage rate of LDH, an important indicator of pyroptosis. Cellular pyroptosis is a type of lytic and inflammatory-dependent programmed cell death that

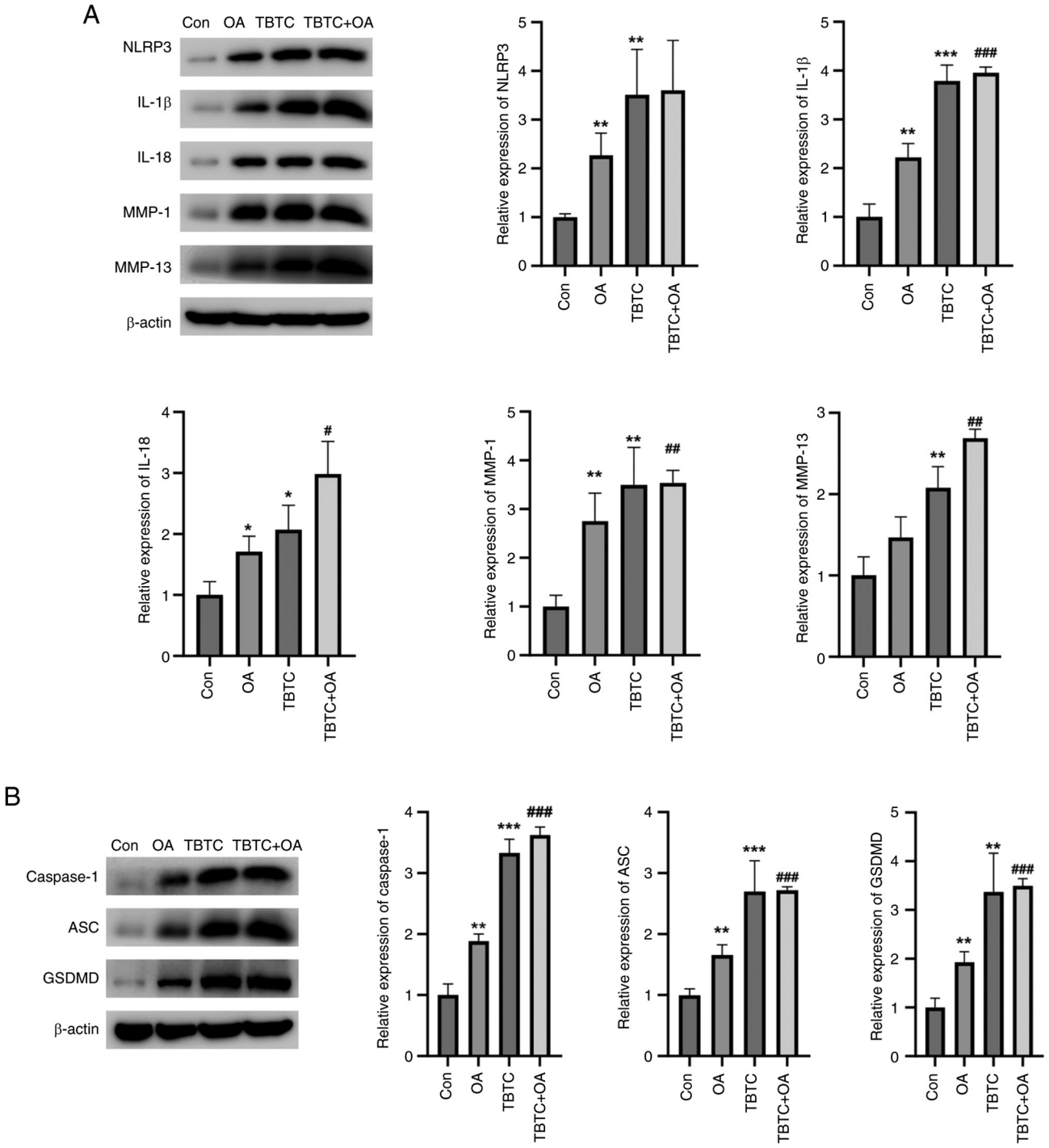

Figure 6. TBTC enhances the NLRP3-mediated inflammatory response and cellular pyroptosis in mouse OA. (A) TBTC increased the protein expression levels of NLRP3, IL-1β, IL-18, MMP-1 and MMP-13. (B) TBTC increased the expression levels of the pyroptosis-related proteins caspase-1, ASC and GSDMD in mouse osteoarticular tissues. *P<0.05, **P<0.01, ***P<0.001 vs. Con; $^{\#}$P<0.05, $^{\#\#}$P<0.01, $^{\#\#\#}$P<0.001 vs. OA. Con. ASC, PYD and CARD domain containing; Con, control; GSDMD, gasdermin D; IL, interleukin; MMP, matrix metalloproteinase; OA, osteoarthritis; TBTC, tributyltin chloride.

leads to the cytolysis and release of inflammatory mediators (IL-1β and IL-18), which then cause tissue damage (4,6,22). Chung *et al* (23) reported that 0.01-0.5 μM TBT induced senescence of human articular chondrocytes *in vitro*. Their results showed that 10 nM TBT reduced human chondrocyte viability and promoted elevated expression of inflammatory factors, but with no statistically significant difference. By contrast, 100 nM TBT significantly induced human chondrocyte senescence and inflammatory responses. Notably, pyroptosis is very similar to apoptosis, but some aspects are markedly different from apoptosis because this death phenomenon is dependent on pro-inflammatory caspase-1. Based on the relationship between pyroptosis and inflammation, a low concentration (25 nM) of TBTC was selected to ensure that it induced an inflammatory response, as well as a high concentration (100 nM) of TBTC, and an intermediate concentration (50 nM) of TBTC. The results revealed that the protein expression levels of IL-1β, IL-18, MMP-1 and MMP-13

were significantly increased in rat chondrocytes after TBTC treatment, indicating that TBTC may induce the release of inflammatory mediators in rat chondrocytes by activating the NLRP3 inflammasome.

Inflammation caused by activation of the NLRP3 inflammasome is the basis of numerous diseases, such as breast cancer and acute liver injury (6,24,25). Once activated, NLRP3 interacts with the adaptor ASC, which subsequently causes the activation of caspase-1 (6). GSDMD, a member of the GSDM family, is cleaved by caspase-1 and releases the N-terminal structural domain, which oligomerizes at the plasma membrane and forms a pore for the release of substrates, such as IL-1β and IL-18 (22,26). Caspase-1-mediated cellular death serves a role in the regulation of various diseases, such as cancer, cardiac hypertrophy and neurological disorders (27-29). In addition, caspase-1 deficiency reduces arthropathic changes in chronic arthritis (30). In the present study, in rat chondrocytes, TBTC was able to increase the expression levels of caspase-1, GSDMD and ASC. To further validate that TBTC activates the upregulation of inflammatory factors in chondrocytes and triggers pyroptosis through activation of the NLRP3 inflammasome, chondrocytes were transfected with a siRNA specifically targeting NLRP3. The results showed that silencing NLRP3 effectively reversed TBTC-mediated increases in the expression of caspase-1, GSDMD and ASC. Therefore, it was hypothesized that TBTC enhanced the expression of the inflammatory factors IL-1β and IL-18 through upregulation of the NLRP3/caspase-1 pyroptosis pathway, causing further expansion of the inflammatory response.

OA is a progressive joint disease, and drugs currently used in the clinic, such as acetaminophen and nonsteroidal anti-inflammatory drugs, can alleviate pain but cannot cure the disease (9). The NLRP3 inflammasome has been shown to be associated with the pathogenesis of various arthritic diseases by stimulating inflammatory mediators and degradative enzymes (9,31). It has previously been reported that the NLRP3 inflammasome serves an important role in inflammation and apoptosis of fibroblast-like synoviocytes, suggesting that the NLRP3 inflammasome is involved in the progression of OA (32,33). Since TBTC can activate the NLRP3 inflammasome-mediated inflammatory response and cellular pyroptosis in chondrocytes, the present study aimed to assess whether TBTC can aggravate the progression of OA. To evaluate this, a mouse model of OA was constructed and the mice were treated with TBTC. Chung *et al* (23) reported that 5 and 25 μg/kg/day TBTC induced mouse articular cartilage aging *in vivo*. This previous study revealed that 25 μg/kg/day TBTC significantly induced aging of joints in mice; however, at 5 μg/kg/day, there was no significant senescence of articular cartilage in mice, but the inflammatory response showed an increased trend. The reason why a high dose of TBTC was not used in the present study is that 25 μg/kg/day TBT induced chondrocyte senescence, which itself causes senescence-associated secretory phenotype. Unlike the aforementioned study, the present study did not consider whether TBTC induced chondrocyte senescence, but instead the present study explored the effects of TBTC on mouse OA. Therefore a dose slightly higher than 5 μg/kg/day was used to ensure that it enhanced the inflammatory response without inducing senescence, thus providing insight into whether TBTC worsened OA. H&E staining revealed more severe cartilage destruction in the OA + TBTC group than in the OA group, which was accompanied by subchondral bone sclerosis, suggesting that TBTC aggravated cartilage degeneration in the osteoarthritic joints in the OA group. The results of Safranin O-Fast Green and toluidine blue staining showed that the loss of proteoglycan staining was more obvious in the OA + TBTC group than in the control group. These results suggested that TBTC may reduce the amounts of collagen and proteoglycans in articular cartilage tissue, which leads to cartilage destruction and aggravates the progression of OA. Consistent with the results of the *in vitro* study, TBTC treatment further exacerbated the expression levels of NLRP3-mediated inflammatory factors, as well as cellular pyroptosis-related proteins in the joint tissues of mice from the OA group, further confirming that the activation of NLRP3 by TBTC exacerbated the inflammatory response and cartilage tissue damage in the mice from the OA group.

In conclusion, to the best of our knowledge, the present study revealed, for the first time, that TBTC exacerbated the progression of OA *in vivo* by activating the NLRP3 inflammasome-mediated inflammatory response and cellular pyroptosis in chondrocytes. Therefore, TBTC may cause damage to the articular cartilage, and it is thus necessary to strictly control the use of TBT.

Acknowledgements

Not applicable.

Funding

This work was supported by a grant from the Natural Science Foundation of Jiangsu Province (grant no. JZ-2021-087).

Availability of data and materials

The data generated in the present study may be requested from the corresponding author.

Authors' contributions

SX and RM designed the study, performed the experiments, analyzed the data and provided final approval of the version to be published. SX and RM confirm the authenticity of all the raw data. Both authors read and approved the final version of the manuscript.

Ethics approval and consent to participate

The present study was approved by the Animal Ethics Committee at Yangzhou University (approval no. YZ-ja986B; Yancheng, China).

Patient consent for publication

Not applicable.

Competing interests

The authors declare that they have no competing interests.

References

1. Abramoff B and Caldera FE: Osteoarthritis: Pathology, diagnosis, and treatment options. Med Clin North Am 104: 293-311, 2020.
2. Colletti A and Cicero AFG: Nutraceutical approach to chronic osteoarthritis: From molecular research to clinical evidence. Int J Mol Sci 22: 12920, 2021.
3. Hawker GA and King LK: The burden of osteoarthritis in older adults. Clin Geriatr Med 38: 181-192, 2022.
4. Yang J, Hu S, Bian Y, Yao J, Wang D, Liu X, Guo Z, Zhang S and Peng L: Targeting cell death: Pyroptosis, ferroptosis, apoptosis and necroptosis in osteoarthritis. Front Cell Dev Biol 9: 789948, 2022.
5. Sharma BR and Kanneganti TD: NLRP3 inflammasome in cancer and metabolic diseases. Nat Immunol 22: 550-559, 2021.
6. Huang Y, Xu W and Zhou R: NLRP3 inflammasome activation and cell death. Cell Mol Immunol 18: 2114-2127, 2021.
7. Fu J and Wu H: Structural mechanisms of NLRP3 inflammasome assembly and activation. Annu Rev Immunol 41: 301-316, 2023.
8. Chen Z, Zhong H, Wei J, Lin S, Zong Z, Gong F, Huang X, Sun J, Li P, Lin H, *et al*: Inhibition of Nrf2/HO-1 signaling leads to increased activation of the NLRP3 inflammasome in osteoarthritis. Arthritis Res Ther 21: 300, 2019.
9. Li X, Mei W, Huang Z, Zhang L, Zhang L, Xu B, Shi X, Xiao Y, Ma Z, Liao T, *et al*: Casticin suppresses monoiodoacetic acid-induced knee osteoarthritis through inhibiting HIF-1α/NLRP3 inflammasome signaling. Int Immunopharmacol 86: 106745, 2020.
10. Zu Y, Mu Y, Li Q, Zhang ST and Yan HJ: Icariin alleviates osteoarthritis by inhibiting NLRP3-mediated pyroptosis. J Orthop Surg Res 14: 307, 2019.
11. Jin X, Dong X, Sun Y, Liu Z, Liu L and Gu H: Dietary fatty acid regulation of the NLRP3 inflammasome via the TLR4/NF-κB signaling pathway affects chondrocyte pyroptosis. Oxid Med Cell Longev 2022: 3711371, 2022.
12. Daigneault BW and de Agostini Losano JD: Tributyltin chloride exposure to post-ejaculatory sperm reduces motility, mitochondrial function and subsequent embryo development. Reprod Fertil Dev 34: 833-843, 2022.
13. Chen P, Song Y, Tang L, Zhong W, Zhang J, Cao M, Chen J, Cheng G, Li H, Fan T, *et al*: Tributyltin chloride (TBTCL) induces cell injury via dysregulation of endoplasmic reticulum stress and autophagy in Leydig cells. J Hazard Mater 448: 130785, 2023.
14. Zhao C, Zhang Y, Suo A, Mu J and Ding D: Toxicity of tributyltin chloride on haarder (Liza haematocheila) after its acute exposure: Bioaccumulation, antioxidant defense, histological, and transcriptional analyses. Fish Shellfish Immunol 130: 501-511, 2022.
15. Horie Y, Yamagishi T, Shintaku Y, Iguchi T and Tatarazako N: Effects of tributyltin on early life-stage, reproduction, and gonadal sex differentiation in Japanese medaka (Oryzias latipes). Chemosphere 203: 418-425, 2018.
16. Pitcher T, Sousa-Valente J and Malcangio M: The monoiodoacetate model of osteoarthritis pain in the mouse. J Vis Exp: 53746, 2016.
17. Livak KJ and Schmittgen TD: Analysis of relative gene expression data using real-time quantitative PCR and the 2(-Delta Delta C(T)) method. Methods 25: 402-408, 2001.
18. Barbosa KL, Dettogni RS, da Costa CS, Gastal EL, Raetzman LT, Flaws JA and Graceli JB: Tributyltin and the female hypothalamic-pituitary-gonadal disruption. Toxicol Sci 186: 179-189, 2022.
19. de Araújo JFP, Podratz PL, Merlo E, Sarmento IV, da Costa CS, Niño OMS, Faria RA, Freitas Lima LC and Graceli JB: Organotin exposure and vertebrate reproduction: A review. Front Endocrinol (Lausanne) 9: 64, 2018.
20. Ximenes CF, Rodrigues SML, Podratz PL, Merlo E, de Araújo JFP, Rodrigues LCM, Coitinho JB, Vassallo DV, Graceli JB and Stefanon I: Tributyltin chloride disrupts aortic vascular reactivity and increases reactive oxygen species production in female rats. Environ Sci Pollut Res Int 24: 24509-24520, 2017.
21. Yao W, Wei X, Guo H, Cheng D, Li H, Sun L, Wang S, Guo D, Yang Y and Si J: Tributyltin reduces bone mineral density by reprograming bone marrow mesenchymal stem cells in rat. Environ Toxicol Pharmacol 73: 103271, 2020.
22. An S, Hu H, Li Y and Hu Y: Pyroptosis plays a role in osteoarthritis. Aging Dis 11: 1146-1157, 2020.
23. Chung YP, Weng TI, Chan DC, Yang RS and Liu SH: Low-dose tributyltin triggers human chondrocyte senescence and mouse articular cartilage aging. Arch Toxicol 97: 547-559, 2023.
24. Faria SS, Costantini S, de Lima VCC, de Andrade VP, Rialland M, Cedric R, Budillon A and Magalhães KG: NLRP3 inflammasome-mediated cytokine production and pyroptosis cell death in breast cancer. J Biomed Sci 28: 26, 2021.
25. Yu C, Chen P, Miao L andf Di G: The role of the NLRP3 inflammasome and programmed cell death in acute liver injury. Int J Mol Sci 24: 3067, 2023.
26. Zhang L, Xing R, Huang Z, Zhang N, Zhang L, Li X and Wang P: Inhibition of synovial macrophage pyroptosis alleviates synovitis and fibrosis in knee osteoarthritis. Mediators Inflamm 2019: 2165918, 2019.
27. Li S, Sun Y, Song M, Song Y, Fang Y, Zhang Q, Li X, Song N, Ding J, Lu M and Hu G: NLRP3/caspase-1/GSDMD-mediated pyroptosis exerts a crucial role in astrocyte pathological injury in mouse model of depression. JCI Insight 6: e146852, 2021.
28. Yan H, Luo B, Wu X, Guan F, Yu X, Zhao L, Ke X, Wu J and Yuan J: Cisplatin induces pyroptosis via activation of MEG3/NLRP3/caspase-1/GSDMD pathway in triple-negative breast cancer. Int J Biol Sci 17: 2606-2621, 2021.
29. Wang F, Liang Q, Ma Y, Sun M, Li T, Lin L, Sun Z and Duan J: Silica nanoparticles induce pyroptosis and cardiac hypertrophy via ROS/NLRP3/Caspase-1 pathway. Free Radic Biol Med 182: 171-181, 2022.
30. Liu J, Jia S, Yang Y, Piao L, Wang Z, Jin Z and Bai L: Exercise induced meteorin-like protects chondrocytes against inflammation and pyroptosis in osteoarthritis by inhibiting PI3K/Akt/NF-κB and NLRP3/caspase-1/GSDMD signaling. Biomed Pharmacother 158: 114118, 2023.
31. Zhang Y, Yan H, Jiang Y, Chen T, Ma Z, Li F, Lin M, Xu Y, Zhang X, Zhang J and He H: Long non-coding RNA IGF2-AS represses breast cancer tumorigenesis by epigenetically regulating IGF2. Exp Biol Med (Maywood) 246: 371-379, 2021.
32. Sakalyte R, Denkovskij J, Bernotiene E, Stropuviene S, Mikulenaite SO, Kvederas G, Porvaneckas N, Tutkus V, Venalis A and Butrimiene I: The expression of inflammasomes NLRP1 and NLRP3, toll-like receptors, and vitamin D receptor in synovial fibroblasts from patients with different types of knee arthritis. Front Immunol 12: 767512, 2022.
33. Zhao LR, Xing RL, Wang PM, Zhang NS, Yin SJ, Li XC and Zhang L: NLRP1 and NLRP3 inflammasomes mediate LPS/ATP-induced pyroptosis in knee osteoarthritis. Mol Med Rep 17: 5463-5469, 2018.